CONF-9510226--2

BNL -62601

Pres. Conf. on Neutrons in Biology,
24-28 October 1994, Santa Fe, NM

HIGH PRECISION THERMAL NEUTRON DETECTORS*

V. Radeka, N. A. Schaknowski, G. C. Smith, and B. Yu

Brookhaven National Laboratory
Upton, NY 11973-5000

October, 1994

*This research was supported in part by the U. S. Department of Energy: Contract No. DE-AC02-76CH00016.

BNL-62601

HIGH PRECISION THERMAL NEUTRON DETECTORS

V. Radeka, N.A. Schaknowski, G.C. Smith and B. Yu
Brookhaven National Laboratory, NY 11973-5000

Abstract

Two-dimensional position sensitive detectors are indispensable in neutron diffraction experiments for determination of molecular and crystal structures in biology, solid-state physics and polymer chemistry. Some performance characteristics of these detectors are elementary and obvious, such as the position resolution, number of resolution elements, neutron detection efficiency, counting rate and sensitivity to gamma-ray background. High performance detectors are distinguished by more subtle characteristics such as the stability of the response (efficiency) versus position, stability of the recorded neutron positions, dynamic range, blooming or halo effects. While relatively few of them are needed around the world, these high performance devices are sophisticated and fairly complex; their development requires very specialized efforts. In this context, we describe here a program of detector development, based on ^{3}He filled proportional chambers, which has been underway for some years at Brookhaven. Fundamental approaches and practical considerations are outlined that have resulted in a series of high performance detectors with the best known position resolution, position stability, uniformity of response and reliability over time, for devices of this type.

1. Introduction

An important role is played by position-sensitive neutron detectors in experiments which use thermal neutrons from reactors or spallation sources, particularly neutron scattering studies of biological, physical and chemical samples. The main nuclei whose neutron cross-sections are large enough to make them suitable choices for neutron detectors are: ^{3}He, used solely in gas proportional detectors, ^{6}Li, used as a thin converter foil or in scintillators such as LiF and LiI, ^{10}B used as a thin converter foil or in the form of BF_3 in gas proportional detectors, and ^{155}Gd, ^{157}Gd or natural Gd, used as a converter foil or as a partial constituent of a phosphor. Thermal neutron detection is based on nuclear reactions, whose products determine the ultimate position resolution of the detector, but the choice of detector technology for a particular application is determined by the experimenter's requirements with respect to additional detector characteristics, such as efficiency, counting rate capability, required size, whether or not dynamic studies are to be performed, sensitivity to background radiation such as gamma-rays, and position stability as a function of time.

A program of detector development for thermal neutron scattering experiments in the study of biological structures has been underway for some years at Brookhaven. The technology of choice has been the gas proportional detector, with ^{3}He as the neutron absorbing gas, because of several beneficial factors. These detectors offer superior efficiency to that of all other detectors, their maximum counting rate capability is adequate for that required in most reactor and spallation source applications, they can be built in a wide range of sizes, they are very insensitive to gamma radiation with appropriate choice of gas mixture, and their position stability is better than most other detectors. In single neutron counting mode, they offer infinite dynamic range for static experiments, while also offering the capability of performing dynamic studies with time frames below one second. We now describe some of the basic characteristics of these gas proportional detectors.

2. Position Resolution and Efficiency

a) Position Resolution

The reaction by which neutrons are stopped in ^{3}He is:

$$^3\mathrm{He} + \mathrm{n} \rightarrow {}^3\mathrm{H} + \mathrm{p} + 0.764\,\mathrm{MeV}$$

The energetic reaction products, a 191 keV triton and a 573 keV proton, are emitted in opposite directions, as shown schematically in figure 1. The ionization centroid of the two particle tracks is displaced significantly from the neutron interaction position because the proton is more heavily ionizing than the triton, and also has a larger range. It is the displaced centroid which the position-sensitive cathodes of the detector measure, independent of the electronic encoding principle. The loci of centroids from many events describe a sphere; when projected in one dimension, these loci describe a rectangular distribution whose width is equal to the diameter of the sphere. In practice, range straggling of the triton and proton, and electronic noise, introduce a small broadening term, and the re-

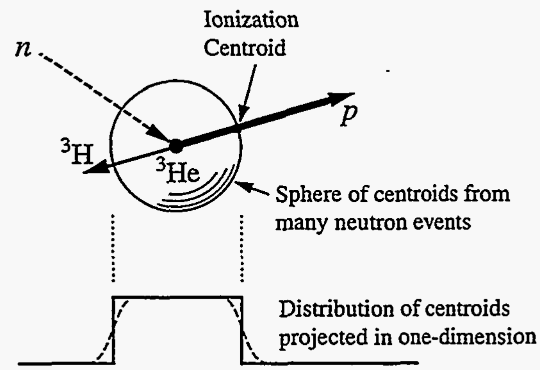

Figure 1. Representation of thermal neutron interaction with ^{3}He nucleus. The reaction products, a triton with kinetic energy 191keV and a proton with kinetic energy 573keV, are emitted in opposite directions. The greater range and ionizing power of the proton results in a displacement of the ionization centroid from the interaction point. Successive events form a sphere of centroids, whose projection in one dimension is a rectangle.

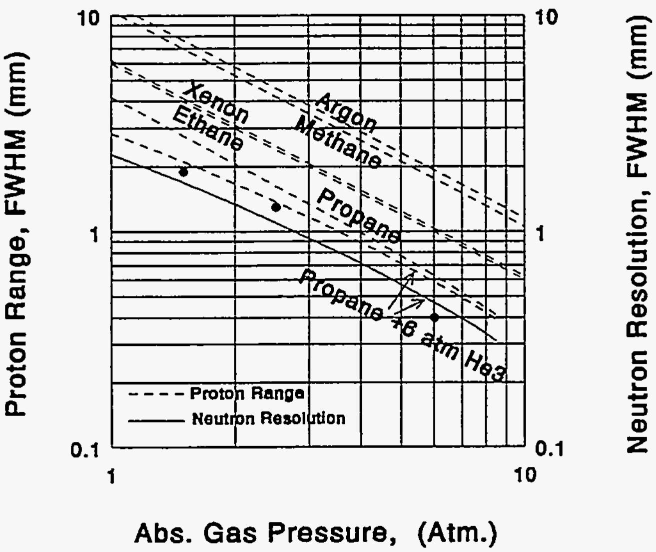

Figure 2. Calculated values for range (dashed lines) of 573keV proton in some suitable gases for admixture with ^3He. Curve for propane decreases more rapidly than 1/pressure because of non-ideal gas behavior. Lower curve (solid line) is predicted resolution for a mixture of 6 atm. ^3He and propane over a range of propane pressures. Solid circles show experimental resolution measurements from operational BNL detectors.

sulting distribution is shown by the dashed lines in figure 1, but the FWHM remains that of the rectangular distribution. It is possible to show that (Fischer, Radeka and Boie, 1983), to a good approximation, the displacement of the total ionization centroid is 0.4 R_p, where R_p is the proton range; thus, the FWHM position resolution is 0.8 R_p.

Proton range, which varies inversely with the density of a particular gas, is several centimeters in 1 atm. He. To achieve resolution in the millimeter range, it is necessary to use an additional gas for the purpose of providing stopping power for the proton and triton. Different gases have been used by various workers to accomplish this task, and the upper five curves in figure 2 show the expected proton range in some suitable gases (Anderson and Ziegler, 1977). From these curves it is clear that propane is an appropriate choice as an additive to ^3He for the proportional chamber gas. Although the higher hydrocarbons have even greater stopping power, there are several reasons that render them unsuitable in this application; they are more likely to form anode wire deposits under intense irradiation, and they are incompatible with most forms of gas purifier (see later). Propane has an additional advantage that its density increases at a slightly greater rate than its pressure (Goodwin and Haynes, 1982). At an absolute pressure of 8.5 atm. its density is about 15% greater than if it were an ideal gas (above 8.5 atm. propane condenses); this phenomenon gives rise to the advantageous deviation from 1/pressure of the proton range curve for propane in figure 2.

b) Efficiency and Gamma Sensitivity

A thermal neutron chamber is, typically, about 1.5 cm deep, and calculations have been carried out to determine the detection efficiency in this gas depth over a range of operating gas pressures. The curves are shown in figure 3, where the lower and upper abscissa have units of Å and meV, respectively, using published cross-section data for ^3He (Garber and Kinsey, 1976). Very high detection efficiencies can be achieved for cold neutrons, around 9Å, with just 1 to 2 atm. of ^3He; as wavelength decreases, efficiency falls, but even at 1 Å an efficiency of about 50% can be achieved with 6 atm. of ^3He. The detection efficiency of this class of detector is significantly greater than that of other detecting media.

As an admixture with ^3He, propane has two advantages in addition to its proton/triton stopping power. First, it is a good quench gas for the proportional avalanche. Second, it has a relatively low photon absorption cross-section. Position sensitive detectors used in neutron scattering studies usually operate in an environment with a high photon background; therefore, the gas added to reduce proton range should have a low sensitivity to X-rays and gamma-rays. Propane has a lower cross-section for gamma-rays than the other four proton stopping gases in figure 2 (Fischer, Radeka and Boie, 1983). Carbon tetrafluoride, not shown in figure 2, has similar stopping power to propane, and has been considered by other groups (Kopp, Valentine, Christophorou and Carter, 1982); however, CF_4 has a somewhat higher photon cross-section, and also is not properly suited to the gas purifier.

3. Basic Operating Principles

A cross-section of the basic proportional chamber structure is shown schematically in figure 4. Neutrons enter through a window, usually aluminum, and most are stopped in the absorption and drift region. The primary ionization created by the proton and triton, about 30,000 electrons, then drifts through the upper wire cathode and an avalanche takes place on the nearest anode wire, or wires. The upper cathode wires and anode wires, though not necessarily of the same pitch, normally run in the same direction. The lower cathode is usually

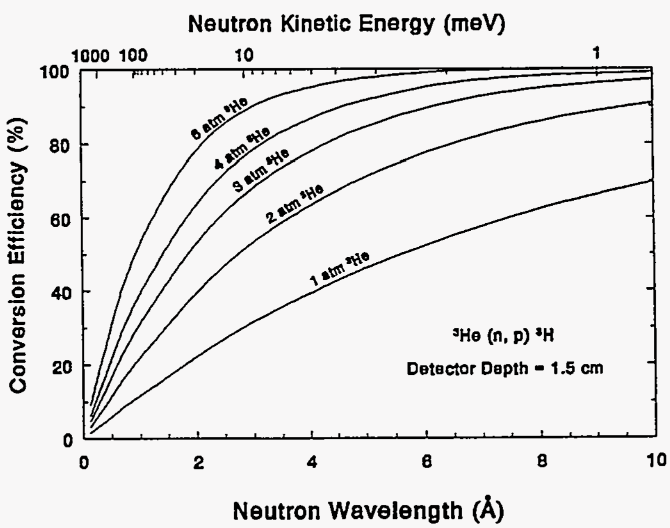

Figure 3. Calculated neutron conversion efficiency for a range of ^3He partial pressures, for a detector with gas depth of 1.5cm. Note that for wavelengths above 1Å, efficiencies of >50% are readily achievable; cold neutron conversion efficiencies are in excess of 80%.

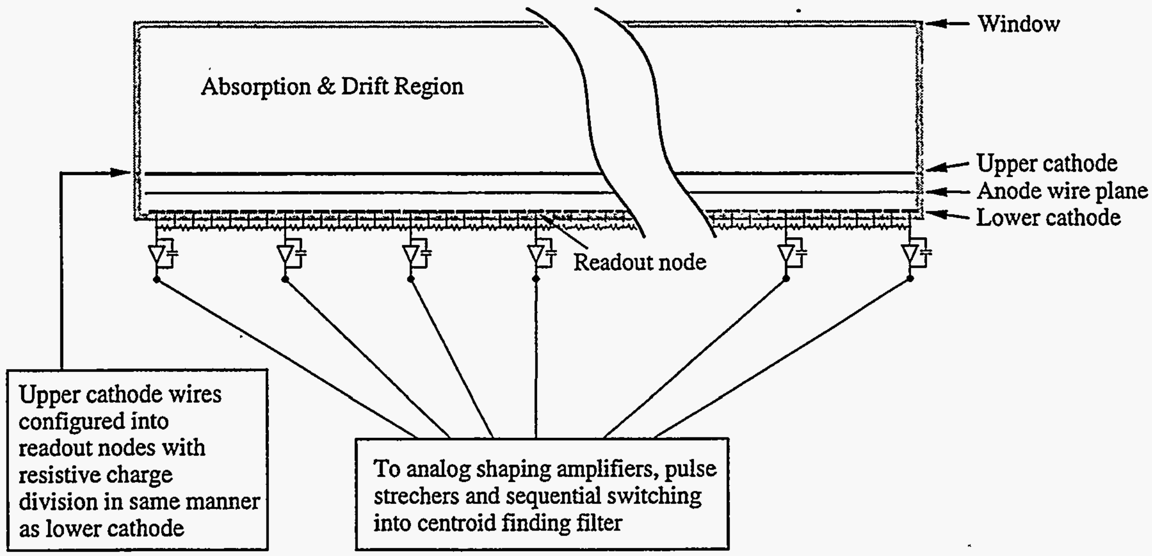

Figure 4. Schematic diagram of proportional chamber geometry. A neutron, entering from top, interacts in the absorption and drift region, secondary ionization then drifts down to the anode. Induced signal charge is collected by two, or three, nodes on each cathode, after resistive charge division; sampled signals are switched to centroid finding electronics.

fabricated on a large glass plate; it has vacuum deposited copper strips, running at right angles to the anode wires. The anode avalanche induces positive charge on both the upper and lower cathodes, with a quasi-Gaussian profile that has a FWHM of approximately 1.5 times the anode-cathode spacing. The sampling of the cathode induced charge with wires or strips yields the center of gravity of the anode avalanche with high precision when appropriate design criteria are followed (Gatti, Longoni, Okuno and Semenza, 1976; Mathieson and Smith, 1989). For convenience, the lower cathode is designated the X-axis and the upper cathode the Y-axis; the anode wires, which are all connected together, yield the total energy signal which is used for gating the position encoding electronics to further eliminate gamma-rays.

Each cathode has a number of readout nodes, connected to charge sensitive preamplifiers. Charge division between nodes is carried out resistively. For combined optimization of position linearity and position resolution, the RC time constant of one subdivision is approximately equal to the shaping amplifier time constant. The anode avalanche from each detected neutron gives rise to collected charge on two, or three, adjacent cathode nodes; these signals are then switched sequentially into a centroid finding filter which yields a timing signal commensurate with the linear position along the respective axis that the event occurred (Radeka and Boie, 1980; Boie et al., 1982). The method achieves a high absolute position accuracy and a high position resolution with small avalanche size because of the number of signal outputs from the detector. The position resolution limit due to electronic noise is given approximately by

$$\mathrm{FWHM} \approx 7\,(kTC_D)^{1/2}(l/N^{3/2})(1/Q_s)$$

where k is Boltzmann's constant, T is absolute temperature, C_D is the total readout electrode capacitance, l the detector length, N the number of subdivisions and Q_s the charge induced on the readout cathode. It is important to note that larger area detectors can be fabricated with the same electronic noise as smaller ones just by using additional nodes and keeping the node spacing, l/N, constant; this major attribute is not possible in global RC encoding methods with only two outputs per axis.

4. Design and Fabrication Details

Detectors with sensitive areas ranging from 5cm×5cm to 50cm×50cm have been designed and fabricated in our detector development program. One device with a sensing area of 20cm×20cm, for example, is housed in a robust aluminum enclosure, consisting of a 38cm diameter base plate, 3cm thick, upon which the electrodes comprising the two cathode and anode planes are mounted. A front cover is bolted to the base, and a double O-ring seal between these two halves serves to provide gas containment. The 20cm×20cm window, machined into the front cover, has a thickness of about 9mm. All electrical feedthroughs are positioned on the thick base plate and are doubly sealed. The enclosure has a maximum allowable operating pressure in excess of 10 atm. absolute. Figure 5 shows a front view of an array of three of these detectors, recently completed for installation in the macromolecular neutron crystallography beam line of Brookhaven's High Flux Beam Reactor (HFBR).

Inside each 20cm×20cm detector, the X-cathode consists of 134 copper strips on a pitch of 1.6 mm. Every seventh strip forms a readout node, connecting to a charge preamplifier, as shown in figure 4. There are 20 nodes on this axis. The Y-cathode consists of wires with a pitch of 0.8mm, electrically connected in pairs; every seventh pair forms a readout node, of which there are 17 on this axis. Figure 6 shows a section along the edge of the X-axis, each node being fed to its corresponding preamplifier (on the outside of the housing) via the glass-to-metal feedthroughs. Chip resistors for the inter-node charge division are positioned between each cathode strip. The anode plane consists of 112 Au plated tungsten wires, with a

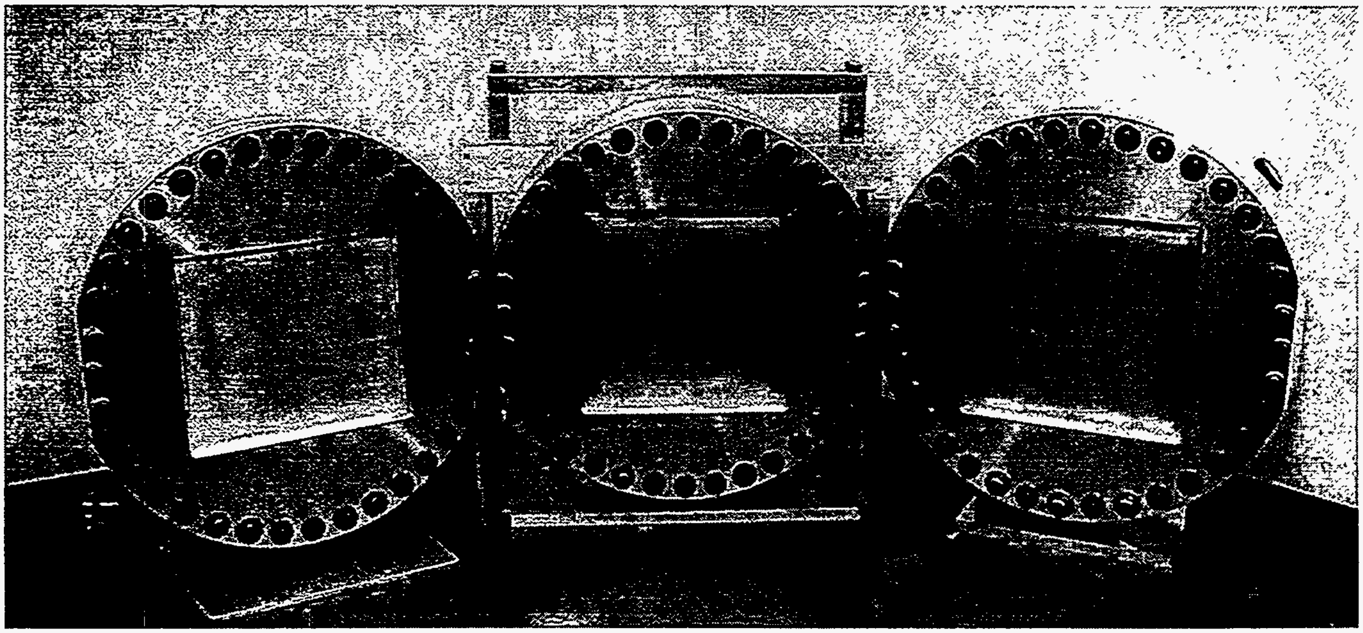

Figure 5. Array of three detectors, each with 20cm×20cm sensitive area, built to upgrade HFBR protein crystallography spectrometer, which previously had just a single detector. This triples the spectrometer's acceptance range and significantly decreases data collection time for structure determination.

diameter of 12mm and a pitch of 1.6mm. There are two guard wires of larger diameter at each side of the anode plane to reduce the electric field.

In the set of detectors constructed in our program, two additional sizes have been fabricated. Most recently, a very high resolution device with a sensitive area 5cm×5cm was completed for an HFBR experiment investigating Rayleigh-Bénard convection, which required position resolution of less than half a millimeter. This was achieved primarily by a combination of the required high pressure to limit the proton/triton range (8 atmospheres of ^{3}He and 6 atmospheres of propane) and reduced node spacing on each position sensing axis. It was also necessary to employ electrode separations and wire spacings of less than 1mm. A picture of the completed detector, taken from the rear, is shown in figure 7; the array of hybrid preamplifier cards for readout of the cathodes can be seen in the electronics housing. A very large area device, 50cm×50cm, has

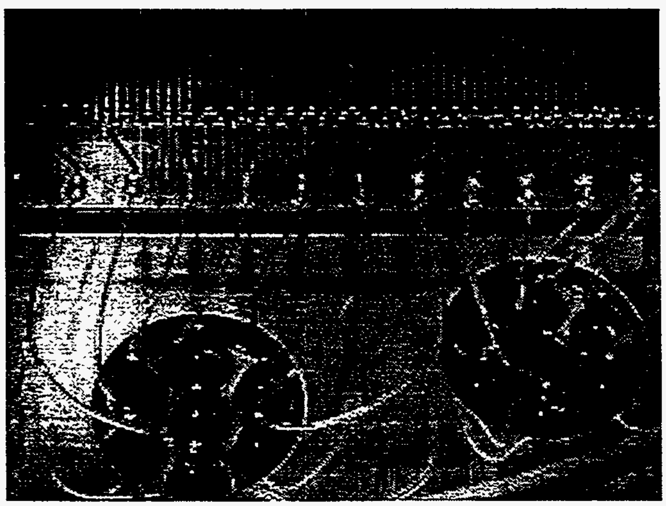

Figure 6. Close-up photograph along edge of lower cathode of 20cm×20cm neutron detector. In upper part, running left to right, are last few wires of upper cathode and anode planes, below which are copper strips of lower cathode running at right angles. Chip resistors between ends of strips form RC network for charge division. Cathode nodes are connected to preamplifiers (not shown) on outside of detector housing, via the glass-to-metal feedthroughs.

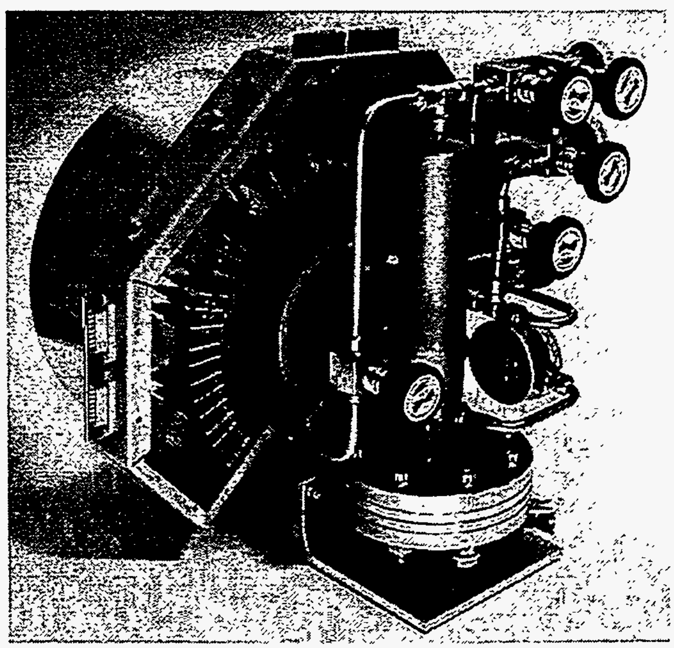

Figure 7. Photograph of rear of the very high resolution detector. With a gas filling of 8 atm. ^{3}He and 6 atm. propane, this detector has achieved the best resolution ever measured in a gas-filled thermal neutron detector, less than 400 μm FWHM. The gas circulation pump is contained in the UHV flange assembly; above this, the vertical cylinder contains the gas purifier.

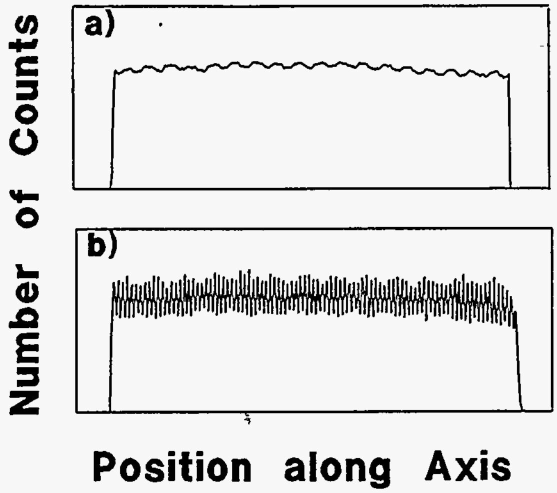

Figure 8. Uniform irradiation responses from 20cm×20cm detector. a) the lower cathode, x-axis response, and b) the upper cathode, Y-axis response.

been in operation for several years at the small angle scattering beam line of the HFBR. This device has a more modest resolution requirement, about 3mm FWHM.

Detectors of this nature, which are fabricated with small quantities of organic materials, will operate over long periods of time only if measures are taken to keep the gas mixture free from impurities. A closed loop gas purification and circulation system is a sensible solution to this problem, bearing in mind the expense of ^3He, about \$150 per STP liter. A small pump, enclosed by a pair of stainless steel UHV flanges, circulates the gas through the detector and a purifier at a rate of approximately 1-2 liters/min. The purifier consists of a stainless steel cylinder with one half length filled with Ridox (Fisher Scientific Co., Fair Lawn, NJ 07410), an oxygen absorber, and the other half length filled with a 3 Å pore size molecular sieve material, mainly for water absorption. The pump and purifier can be seen on the detector assembly in figure 7. This arrangement permits limited use of chamber construction materials such as G10 fiberglass. The purifier has been very effective in maintaining a high level of purity in the gas mixture: most detectors constructed in this program have operated without interruption for several years.

5. Operating Characteristics

A sensitive measure of linearity can be achieved by irradiating the detector with a beam of neutrons of uniform intensity per unit area, and measuring the position spectrum. Figure 8(a) and (b) show the X-axis and Y-axis responses, respectively, from the 20cm×20cm detector. In the X-axis there is a small, residual modulation whose magnitude is small, about ±3%, and which is due to the inter-node charge division. The modulation has a periodicity equal to the node spacing and is extremely stable. In the Y-axis, there is a modulation due to the discrete anode wire locations. This again is very stable.

Position resolution has been determined by measuring detector response to a finely collimated beam of neutrons incident normally on the window. In figure 2 are shown

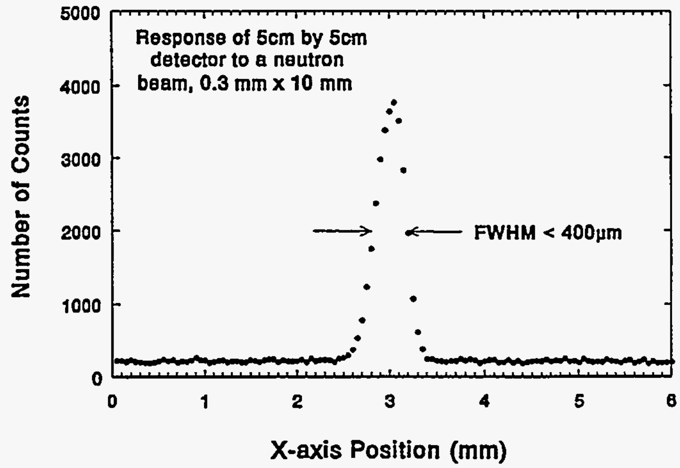

Figure 9. Position response from the very high resolution detector.

experimental measurements (solid circles) for three different propane pressures: 1.5, 2.5 and 6 atm. The first two are taken with the 20cm×20cm detector with an additional 4 atm. ^3He, and the third was taken with the 5cm×5cm detector with an additional 8 atm. ^3He. The solid curve in figure 2 is the predicted resolution for a mixture of 6 atm. ^3He with a range of propane pressures (since ^3He has a relatively small influence on proton range, its partial pressure has only a small effect on the predicted resolution). These measurements have been performed under normal operating conditions of the detectors, with almost no contribution to position resolution from electronic noise. There is good agreement between measured and predicted resolution. To our knowledge, the data point at 6 atm. propane, corresponding to a FWHM <400 μm, is the best resolution ever recorded in a gas-filled thermal neutron detector; the corresponding position distribution is shown in figure 9.

A measure of absolute position accuracy is shown in figure 10, which is the response of the large 50cm×50cm detector to a raster scan of 36 primary beams of thermal neutrons. The excellent absolute accuracy is illustrated by the similarity of peaks in a particular row and a particular column.

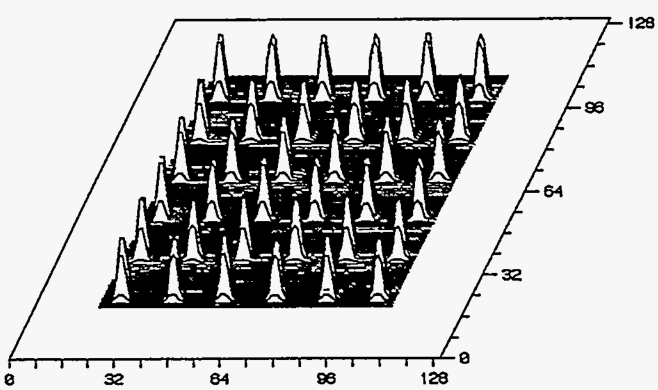

Figure 10. Response of the 50cm×50cm detector to a raster scan of 36 primary neutron beams, illustrating the excellent absolution position accuracy of these detector systems (from Schoenborn, Schefer and Schneider, 1986).

Table 1: Performance Figures

Position Resolution (FWHM)	<0.4 - 2 mm
Number of Resolution Elements	from 128×128 to 1024×1024
Size	from 5×5 cm^2 to 50×50 cm^2
Wavelength Range	1 - 20 Å
Detection Efficiency	50 - 80 %
Counting Rate (total)	10^5 - 5×10^5 sec^{-1} (single readout)
Counting Rate (single peak)	5×10^4 sec^{-1}
Integral non-linearity	2×10^{-4} to 10^{-3}
Absolute Position Accuracy	30-100 µm
Stability of Origin	<50 µm
Stability of Response (efficiency)	<1%
Differential non-linearity	±3%
Dynamic Range	Single Neutron Detection
Timing Resolution	<250 ns

A useful summary of operating characteristics of gas filled proportional chambers for thermal neutron detection is given in table 1. It should be noted that not all the properties listed can necessarily be achieved in one detector at the same time.

6. Concluding Remarks

A set of detectors has been designed and fabricated which provide high resolution, stable, and reliable performance to a range of structural biology experiments, in particular those at the Brookhaven's HFBR. In this ongoing program, new devices and techniques are under development; for example, methods to minimize parallax errors in planar detectors for small angle experiments are being investigated, and large, curved detectors for crystallography experiments are being studied. Finally, it should be emphasized that the proportional detectors described here have one important advantage over competing devices such as image plates and phosphor/CCDs: the proportional detector, with sub-microsecond timing resolution, is the only device from these three with adequate timing resolution for white beam experiments at spallation sources.

Acknowledgments

We wish to acknowledge the invaluable contributions to this detector development program made by Joachim Fischer, who passed away in 1995. We are indebted to Joe Mead and Frank Densing for fabrication and testing of the analysis electronics. We have had very helpful advice and feedback from colleagues working in Structural Biology, in particular Richard Korszun, Anand Saxena and Dieter Schneider at Brookhaven, and Benno Schoenborn at Los Alamos. This research was supported by the U.S. Department of Energy: Contract No. DE-AC02-76CH00016.

References:

Anderson, H.H., and Ziegler, J.F., 1977, Hydrogen Stopping Power and Ranges in All Elements, *Vol. 3, Pergamon Press, New York.*

Boie, R.A., et al., 1982, Two-Dimensional High Precision Thermal Neutron Detectors, *Nucl. Instrum. & Meth.* 200: 533-545.

Fischer, J., Radeka, V. and Boie, R.A., 1983, High Position Resolution and Accuracy in He^3 Two-dimensional Thermal Neutron Detectors. *Workshop on The Position-Sensitive Detection of Thermal Neutrons, ILL, Grenoble, France 11-12 October 1982. Proceedings edited by P. Convert and J.B. Forsyth (Academic Press, London)*, p129.

Garber, D.I., and Kinsey, R.R., 1976, Neutron Cross Sections Volume II, Curves, *Report No. BNL 325. Brookhaven National Laboratory.*

Gatti, E., Longoni, A., Okuno, H., and Semenza, P., 1979, Optimum Geometry for Strip Cathode or Grids in MWPC for Avalanche Localization along the Anode Wires, *Nucl. Instrum. & Meth.* 163: 83-92.

Goodwin, R.D., and Haynes, W.M, 1982, Thermophysical Properties of Propane from 85 to 700 °K at Pressures to 70 MPa. *U.S. Dept. of Commerce, National Bureau of Standards.*

Kopp, M.K., Valentine, K.H., Christophorou L.G., and Carter, J.G., 1982, New Gas Mixture Improves Performance of He^3 Neutron Counters. *Nucl. Instrum. & Meth.* 201: 395-401.

Mathieson, E., and Smith G.C., 1989, Reduction in non-linearity in Position-sensitive MWPCs. *IEEE Trans. Nucl. Sci.* NS-36: 305-310.

Radeka, V. and Boie, R.A., 1980, Centroid Finding Method for Position-Sensitive Detectors, *Nucl. Instrum. & Meth.* 178: 543-554.

Schoenborn, B.P., Schefer, J., and Schneider, D.K., 1986, The Use of Wire Chambers in Structural Biology, *Nucl. Instrum. & Meth.* A252: 180-187.